LOAD TRANSFER IN A GRAPHENE/PDMS NANOCOMPOSITE UNDER NANOINDENTATION

Guoxin Cao[1],Tianxiao Niu[2] and Chunyang Xiong[3]

[1] Department of Mechanics & Engineering Science, Peking University, Beijing, 100871, China, Caoguoxin@pku.edu.cn
[2] Department of Mechanics & Engineering Science, Peking University, Beijing, 100871, China, niutianxiaoheu@163.com
[3] Department of Mechanics & Engineering Science, Peking University, Beijing, 100871, China, cyxiong@pku.edu.cn

Key Words: AFM indentation, mechanical properties, graphene/PDMS nanocomposite

Abstract
Indentation response of graphene/PDMS nanocomposite (graphene monolayer mounted on PDMS substrate) performed by atomic force microscopy (AFM) is investigated by both experiments and computational simulations, which is significantly different from that of most materials or structures. Appearance of PDMS substrate is invisible to the deformation of graphene which is exactly analogous to that of free-standing (F-S) graphene in indentation tests but just with a smaller indentation depth; the screening effect of the AFM tip is created by graphene, which causes that the AFM tip geometry is invisible to the PDMS substrate (or insensitive to the tip geometry). The main reasons are the huge membrane/substrate elastic modulus ratio (~10^6) and the very large ratio of indentation depth to membrane thickness (~10^3). The interface between graphene and PDMS is not failed even with the maximum strain of 5% in graphene, which is significantly higher than the reported maximum strain transferred between graphene and substrate.

1. Introduction

Since 2D materials are typically only in atomic-level thick, their elastic modulus are typically measured based on their indentation responses. There are two types of indentation tests: (I) free standing indentation (FSI) tests performed by AFM,[1-5] in which the tested graphene is suspended on the substrate hole, in other words, there is no substrate beneath the indentation point (or the elastic modulus of substrate is considered to be infinitesimal); (II) conventional indentation (CI) tests performed by commercial nanoindentor,[6, 7] in which graphene is mounted on the common substrate (e.g., SiO_2 or poly(ethylene terephthalate) (PET), with the elastic modulus of around 70 and 3.7 GPa, respectively).

In CI tests, the overall reduced modulus (E') of 2D material and its substrate can be determined from the measured P-δ relationship on the basis of the Oliver-Pharr method[8], and then, E_g is determined from overall P-δ relationship after decoupling the contribution of substrate (E_s) from the following model:[9]

$$\frac{1}{E'}=\frac{1-\nu_g^2}{E_g}\left(1-e^{-\zeta hA^{-0.5}}\right)+\frac{1-\nu_s^2}{E_s}e^{-\zeta hA^{-0.5}} \quad (1)$$

where ν_f and ν_s are the Poisson's ratios of 2D material and substrate, A is the contact area, h is the thickness of 2D material and ζ is the commercial indenter tip geometric factor (ζ = 1.3). E_g is then

Excerpt from ISBN 978-3-00-053387-7

identified as 0.89 TPa for monolayer graphene,[6] which is about 10% lower than that determined by the FSI tests.
However, the overall P-δ relationship in CI tests might be not good to determine E_g of graphene monolayer since its contribution to E' is very small. In practice, 2D materials are always connected with substrate by van der Waals (vdW) interaction in their applications (e.g., nano-electro-mechanical devices or graphene reinforced polymers). The substrate will restrain the local out-of-plane deformation which occurs in FSI tests and the vdW interaction between the substrate and 2D materials might also affect the mechanical response of graphene, and therefore, the mechanical behavior of graphene determined from the testing environment including substrate will be more effective to help the development of the important application based on 2D materials. In addition, there are also discussions about that the boundary condition and initial condition might not be effectively described in FSI tests.[10-14]

In the present work, the indentation response of graphene monolayer (the strongest membrane) mounted on PDMS (super-soft matter) is measured using AFM, in which the substrate environment is induced and the maximum contribution of graphene to the overall indentation response can be also realized. In addition, the deformation mechanism of graphene/PDMS under AFM indentation is also investigated using FEM.

2. Methods

2.1. Experimental method

In the present work, the nanocomposite is made by a graphene monolayer covered with a super-soft substrate (PDMS) (10×10 mm and the thickness of 2 mm), as shown in Figure 1. A two-component PDMS from Dow Corning (Sylgard^R 184) is selected. The mixing ratio of PDMS base to curing agent is 10:1 and the curing condition is 85℃ for 4h. Monolayer graphene on copper foil grown by chemical vapor deposition (CVD) (ACS Materials, USA) is used. Graphene is transferred to the PDMS substrate following the common procedure reported by Chen et al.[15] The indentation response of graphene/PDMS is measured by AFM, and the AFM tip sizes are characterized as: R = 21, 41 nm in the present work.

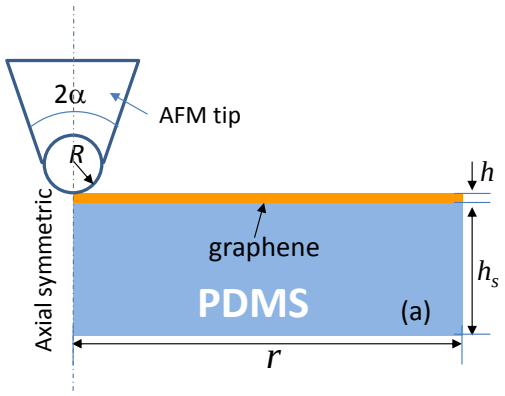

Figure 1. schematic of nanoindentation of graphene/PDMS composite;

2.2 Finite element modeling method

All FEM simulations are carried out using ABAQUS v6.10. In FEM, both sample and AFM tip will be simplified to be axial symmetric, e.g., AFM tip can be considered to be spherical and the sample is modeled as a circular membrane mounted on a cylindrical substrate. Since the thickness of graphene is at atomic level and their bending stiffness is very small, graphene can be modeled by the membrane elements. The AFM tip is considered to be rigid since it is much stiffer than the overall stiffness of graphene/PDMS composite. Since the vdW attraction between graphene and substrate is very strong, graphene is modeled to be perfectly bonded with its substrate. The bottom surface of substrate is

Excerpt from ISBN 978-3-00-053387-7

constrained along the thickness direction (*y*-direction) and is freely deformed along the radial direction (*x*-direction). The adhesion between indenter tip and sample is neglected in the present work and the contact between indenter tip and the top face of sample is considered to be frictionless.

3. Results

3.1. Measured indentation response

Figure 2(a) and 2(b) show the *P*-δ relationships of pure PDMS and graphene/PDMS composite measured using AFM with two different tips. Compared with pure PDMS, the indentation load (*P*) of the graphene/PDMS structure is significantly increased, e.g., the value of *P* is roughly increased by about 10-18 times at δ = 200 nm (a higher increase for a smaller tip). It means that introducing graphene can significantly increase the indentation modulus of PDMS. For both pure PDMS and graphene/PDMS, the indentation deformation can be fully recovered after unloading, which means that their deformations are pure elastic; there is a small difference between the loading and unloading curves (creating a small hysteresis loop) due to the weak viscous feature of PDMS.

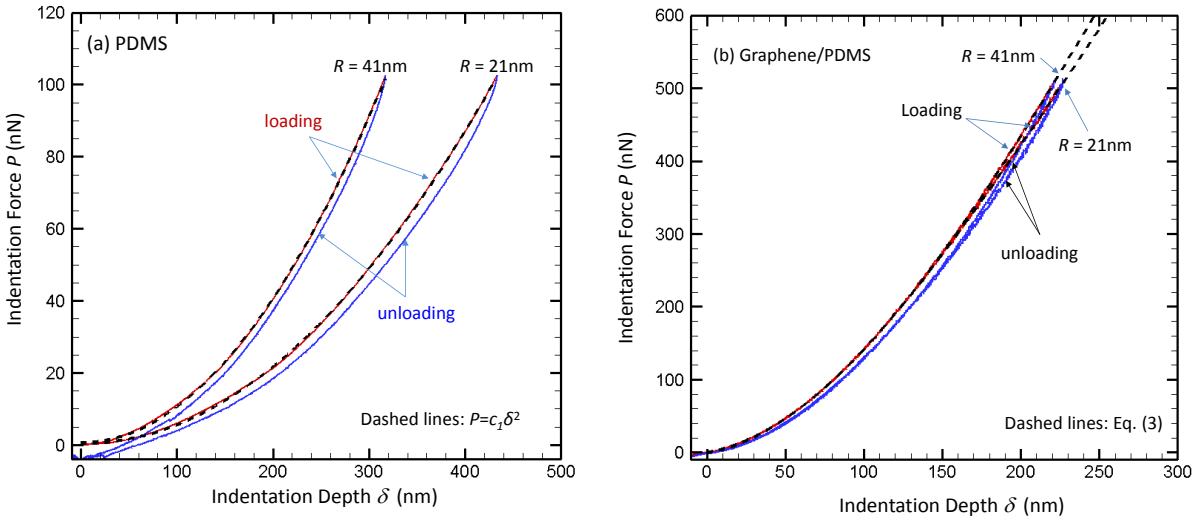

Figure 2. Indentation load-indentation depth (P-δ) relationship measured by AFM with different tips. (a) PDMS; (b) graphene/PDMS composite.

The indentation curves of graphene/PDMS are very smooth (see Figure 2(b)), which indicate that graphene is perfectly bonded with PDMS substrate and there is no slip between graphene and PDMS in indentation (i.e., the graphene/PDMS interface is very strong). If the slippage occurs in the tests, the stiffness of the sample will be sharply change and you will see a small slump in the indentation load (i.e., the indentation curve will not be smooth). Using the geometric feature of the indentation curve to judge whether the slippage occurs in indentation tests is widely used.[1] Graphene monolayer is perfectly bonded with PDMS and the indentation load is fully transferred across the interface, which can be also shown by the tremendously increased value of *P* (up to 18 times).

It is a very interesting finding that the *P*-δ relationships of graphene/PDMS are essentially not sensitive to the tip size *R*: *P* increases by less than 2% with *R* increased twice (at δ = 200 nm), which is significantly different from the CI responses under a spherical tip, but analogous to the FSI results. In CI tests, the *P*-δ relationship of elastic materials under a pyramidal/spherical tip can be described by the following equations, respectively: [8]

$$P = c_1\delta^2 \text{ (pyramidal) and } P = c_2\delta^{1.5} \text{ (spherical)} \quad (2)$$

Excerpt from ISBN 978-3-00-053387-7

where $c_1 \propto E/(1-\nu^2)\tan\theta$ and θ is the equivalent conic half angle of pyramidal tip; $c_2 \propto R^{0.5}E/(1-\nu^2)$, E and ν are the elastic modulus and Poisson's ratio of material measured, e.g., the P-δ curve of pure PDMS follows the first expression of Equation (2) very well (displayed as the dashed lines in Figure 2a). Both of expressions show that P depends upon the tip geometry; whereas P is not related to R in FSI tests. Although the measured P-δ curve of graphene/PDMS composite cannot follow either function type expressed in Equation (2), it can be well fitted as the weighted average of both of them on the basis of the least-square method (displayed as the dashed lines in Figure 2b) :

$$P = A\delta^{1.5} + B\delta^2 \quad (3)$$

in which A and B are the fitting parameters and depend upon the equivalent modulus of graphene/PDMS.

In the range $\delta < 200$ nm, the maximum deviation between the measured P and the corresponding value predicted by Equation (3) is only 1%. Figure 3 show the distributions of A and B of graphene/PDMS composite measured from two different tips. With R increased twice, A and B vary less than 1% and 10%, respectively. Since the second term of Equation (3) only gives a very weak contribution to the overall load (~15% at δ = 200 nm, and slightly increases with δ), the parameters A and B are essentially not sensitive to the value of R (or θ). In addition, the statistic results also show that indentation behavior of graphene/PDMS can be effectively described by Equation (3): A = 0.1202 ± 0.0035 (with the unit of nN/nm$^{1.5}$) and B = (1.85 ± 0.3) × 10^{-3} (with the unit of nN/nm^2) when P and δ are measured in nN and nm; in other words, there is only ~2% fluctuation in P (Although the error range of B is slightly higher, the second term of Equation (3) gives a weak contribution to the overall load).

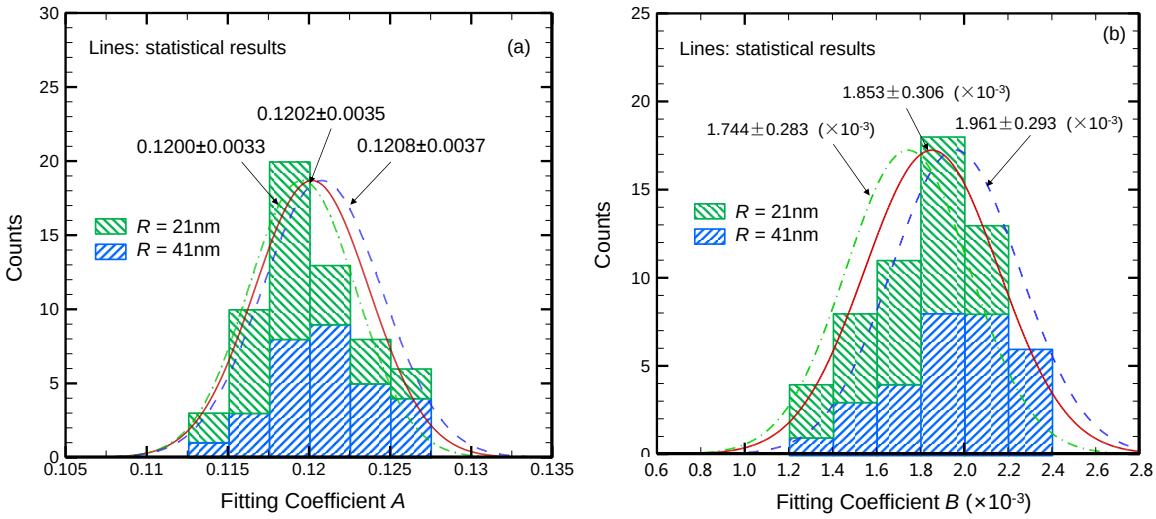

Figure 3. The distribution of the fitting parameters A and B of graphene/PDMS composite measured from two different AFM tips. The solid line shows the overall statistic results of both tips.

3.2. Simulated indentation response

The elastic modulus ratio of graphene (the strongest membrane) to PDMS (the softest material) can be up to ~10^6 and the ratio of indentation depth to membrane thickness reaches to ~10^3, both of which are significantly higher than those of the reported results in CI tests, and thus, the indentation behavior of graphene/PDMS composite should be more complicated. In present work, FEM is employed to understand the deformation mechanism of the indentation response of graphene/PDMS composite. Graphene is typically considered to be nonlinear, i.e., the stress-strain (σ-ε) relationship can be described as: $\sigma = E_g\varepsilon + D_g\varepsilon^2$, where E_g is the second-order elastic modulus of graphene, D_g is the

Excerpt from ISBN 978-3-00-053387-7

third-order nonlinear elastic modulus of graphene (D_g < 0), σ is the 2nd P-K stress and ε is the Lagrangian strain; whereas the nonlinear effect of graphene are commonly neglected when the deformation of graphene is small (e.g., ε < 2%). Thus, the linear elastic model is used for graphene in simulating the indentation response of the graphene/PDMS composite (with a small value of δ). The material properties of graphene monolayer can be selected as E_g = 1.0 TPa, ν_g = 0.17. In addition, according to our experimental results, PDMS can be also modeled as linear elastic material (with E_s = 1.12 MPa, ν_s = 0.49).

The FEM simulation results also show that the P-δ relationship of graphene/PDMS can be well fitted as Equation (3). The appearance of PDMS substrate will not have a noticeable effect on the deformation of graphene, i.e., PDMS is essentially invisible to graphene in the indentation tests. Figure 4(a) shows the FEM result of the defection of graphene in graphene/PDMS under indentation, and the counterpart of graphene in FSI tests (with a = 1 μm) is also displayed in the figure for reference purposes (shown as the dashed line). When the maximum radial strain is matched between two cases mentioned above (ε_{max} at r = 0, as shown in Figure 4(b)), the indentation depth of graphene/PDMS (δ) is much larger than that of F-S graphene ($\delta_{F\text{-}S}$). However, after directly downshifting the deflection profile of F-S graphene to match its maximum deflection with that of graphene/PDMS ($\delta_{F\text{-}S}|_{r=0} = \delta|_{r=0}$), the deflection profiles of two cases agree with each other perfectly. The above result further verified that the deformation of graphene in graphene/PDMS indentation is actually very similar to that in the F-S indentation tests but just with a smaller deflection ($\delta_{F\text{-}S} \approx \delta|_{r=0} - \delta|_{r=1\mu m}$), e.g., $\delta|_{r=0}$ = 240 nm, $\delta|_{r=1\mu m}$ = 122nm. If we approximately consider that the indentation load P of graphene/PDMS is mainly supported by the part of sample with $r \leq 1\mu m$, the contribution of graphene to the indentation load is represented as: $P_g \propto \delta_{F\text{-}S}^3$. FEM also shows that there is roughly a power-law relationship between δ and $\delta_{F\text{-}S}$ ($\delta_{F\text{-}S} \approx \delta|_{r=0} - \delta|_{r=1\mu m}$): $\delta_{F\text{-}S} \approx k\delta^{0.6}$, and thus, $P_g \propto \delta^{1.8}$. If the boundary of a larger area is selected to represent the clamped boundary of F-S graphene (e.g., $\delta_{F\text{-}S} \approx \delta|_{r=0} - \delta|_{r=2\mu m}$), the power parameter in the $\delta_{F\text{-}S}$ -δ relationship (or in P_g-δ) will continually decrease, which can be shown in Figure 4(a). Simultaneously, the deformation of PDMS in the indentation of graphene/PDMS is more like the indentation under a huge conical indenter created by deformed graphene and the real tip geometry is screened by graphene (i.e., the contribution of substrate to the overall indentation load $P_s \propto \delta^{1.5}$ but not depends upon the tip geometry). Since PDMS is super-soft, the appearance of PDMS only causes a vertical shift of the deformation profile of graphene but no effect on radial strain. Therefore, the overall indentation response of graphene/PDMS can be expressed as Equation (3).

It is reported that the maximum strain that can be transferred between stretchable substrate and graphene is less than 1.6%.[16, 17] However, the largest radial strain of graphene created by indentation $\varepsilon_{max} \approx 0.054$ in the graphene/PDMS composite (based on the nonlinear elastic model, see Figure 4(b)), which can be further increased with δ. It is found that the interface between graphene and PDMS is still not failed even with a more than 5% ε_{max} of graphene which can be validated by the smooth P-δ curves of graphene/PDMS measured in experiments (no sign for slippage). This result indicates that the maximum strain transferred between substrate and graphene is strongly dependent upon their elastic modulus ratio.

Excerpt from ISBN 978-3-00-053387-7

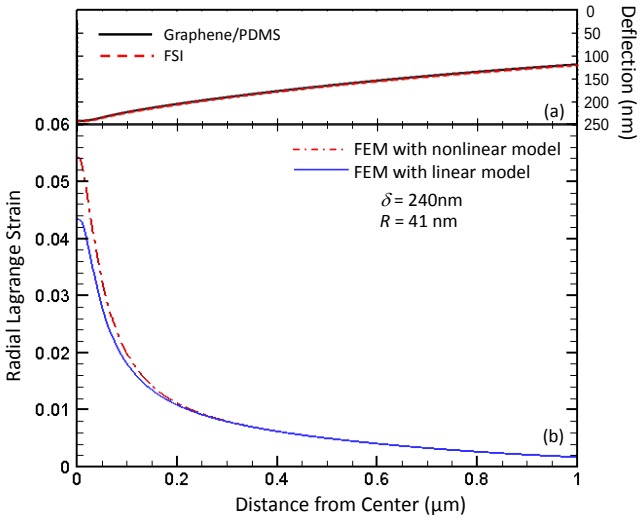

Figure 4. The FEM simulation results of the deformation of graphene along radial direction in the graphene/PDMS composite under spherical indentation with R = 41 nm. (a) the vertical deflection of graphene; (b) the radial strain of graphene calculated based on both the linear and nonlinear elastic models. As a reference, the vertical deflection of graphene in FSI is also displayed in Figure 4(a).

4. Conclusions

The indentation response of the strongest, thinnest membrane mounted on the softest substrate (graphene/PDMS) performed by AFM tip is investigated by both experiments and simulations, which is highly different from that of most reported materials or structures. The main reasons are the super-high membrane/substrate elastic modulus ratio (~10^6) and the high ratio of indentation depth to membrane thickness (~10^3) which are significantly higher than the reported corresponding values. From both experimental and simulation results, the indentation load P is not sensitive to the tip geometry; the P-δ relationship does not follow the conventional function type ($P \propto \delta^2$ or $P \propto \delta^{1.5}$) but perfectly matches with the weighted average of both of them ($P = A\delta^{1.5} + B\delta^2$).

For the composite of graphene/PDMS, the appearance of PDMS substrate is essentially invisible to the deformation of graphene, which is exactly same as that in FSI tests just with a smaller indentation depth. Due to the screening effect of graphene, the indenter tip is also invisible to PDMS substrate and the deformation field of PDMS is much more uniform than that in CI tests (more like the indentation response under a huge indenter tip created by the deformed graphene). In addition, the interface between graphene and PDMS is still not failed even when the maximum strain of graphene is more than 5%, which is significantly higher than the reported maximum strain transferred between graphene and substrate. This result indicates that the maximum strain transferred across the interface is strongly dependent upon the elastic modulus ratio of two phases separated by interface.

References

1. Lee, C., X.D. Wei, J.W. Kysar, and J. Hone, *Measurement of the elastic properties and intrinsic strength of monolayer graphene.* Science, 2008. **321**(5887): p. 385-388.
2. Frank, I.W., D.M. Tanenbaum, A.M. Van der Zande, and P.L. McEuen, *Mechanical properties of suspended graphene sheets.* Journal of Vacuum Science & Technology B, 2007. **25**(6): p. 2558-2561.
3. Lee, G.H., et al., *High-Strength Chemical-Vapor Deposited Graphene and Grain Boundaries.* Science, 2013. **340**(6136): p. 1073-1076.
4. Bertolazzi, S., J. Brivio, and A. Kis, *Stretching and Breaking of Ultrathin MoS2.* Acs Nano, 2011. **5**(12): p. 9703-9709.

Excerpt from ISBN 978-3-00-053387-7

5. Castellanos-Gomez, A., et al., *Elastic Properties of Freely Suspended MoS2 Nanosheets.* Advanced Materials, 2012. **24**(6): p. 772-+.
6. Zhang, Y.P. and C.X. Pan, *Measurements of mechanical properties and number of layers of graphene from nano-indentation.* Diamond and Related Materials, 2012. **24**: p. 1-5.
7. Chen, J., et al., *Nanomechanical properties of graphene on poly(ethylene terephthalate) substrate.* Carbon, 2013. **55**: p. 144-150.
8. Oliver, W.C. and G.M. Pharr, *Measurement of hardness and elastic modulus by instrumented indentation: Advances in understanding and refinements to methodology.* Journal of Materials Research, 2004. **19**(1): p. 3-20.
9. Chen, S.H., L. Liu, and T.C. Wang, *Investigation of the mechanical properties of thin films by nanoindentation, considering the effects of thickness and different coating-substrate combinations.* Surface & Coatings Technology, 2005. **191**(1): p. 25-32.
10. Zhou, L.X., Y.G. Wang, and G.X. Cao, *Boundary condition and pre-strain effects on the free standing indentation response of graphene monolayer.* Journal of Physics-Condensed Matter, 2013. **25**(47): p. 475303.
11. Lu, Z.X. and M.L. Dunn, *van der Waals adhesion of graphene membranes.* Journal of Applied Physics, 2010. **107**(4): p. 044301.
12. Zhou, L.X., Y.G. Wang, and G.X. Cao, *van der Waals effect on the nanoindentation response of free standing monolayer graphene.* Carbon, 2013. **57**: p. 357-362.
13. Zhou, L.X., J.M. Xue, Y.G. Wang, and G.X. Cao, *Molecular mechanics simulations of the deformation mechanism of graphene monolayer under free standing indentation.* Carbon, 2013. **63**: p. 117-124.
14. Cao, G.X., *Atomistic Studies of Mechanical Properties of Graphene.* Polymers, 2014. **6**(9): p. 2404-2432.
15. Chen, X.D., et al., *High-quality and efficient transfer of large-area graphene films onto different substrates.* Carbon, 2013. **56**: p. 271-278.
16. Young, R.J., I.A. Kinloch, L. Gong, and K.S. Novoselov, *The mechanics of graphene nanocomposites: A review.* Composites Science and Technology, 2012. **72**(12): p. 1459-1476.
17. Jiang, T., R. Huang, and Y. Zhu, *Interfacial Sliding and Buckling of Monolayer Graphene on a Stretchable Substrate.* Advanced Functional Materials, 2014. **24**(3): p. 396-402.

Excerpt from ISBN 978-3-00-053387-7